IL NUOVO CIMENTO Vol. 24 C, N. 6 Novembre-Dicembre 2001

Equilibration of a two-level primitive equation model on the sphere(*)

R. Caballero(1), R. Castegini(2) and A. Sutera(2)

(1) *Danish Center for Earth System Science, University of Copenhagen - Denmark*
(2) *Dipartimento di Fisica, Università di Roma "La Sapienza" - Rome, Italy*

(ricevuto il 12 Giugno 2000; revisionato il 30 Marzo 2001; approvato il 17 Maggio 2001)

Summary. — The equilibration of a two-level primitive equation model forced by relaxation towards a fixed axisymmetric temperature profile is studied as a function of the forcing equator-to-pole temperature difference. We find that the mean equilibrated temperature gradient rises quickly with the forcing. It is found also that the mean eddy momentum flux convergence induces a strong barotropic jet at mid-to-high latitudes. We suggest that, as found in previous work, the barotropic governor effect induced by the jet is responsible for the sensitivity of the equilibrated temperature gradient to the forcing.

PACS 92.60.Bh – General circulation.

1. – Introduction

A central but as yet unsettled question in climatology is that of the factors determining the mean observed equator-to-pole temperature gradient. The question, aside from its obvious scientific interest, has practical implications in that a detailed understanding of the underlying mechanisms would presumably lead to an accurate parameterisation for the statistical effect of zonally asymmetric eddies on the atmospheric general circulation, facilitating the development of numerically inexpensive models of the climate system.

One approach to the problem is to consider highly simplified models of the atmosphere where relevant mechanisms may more easily be identified and analysed; one may subsequently assess the relevance of these mechanisms using observations or GCM-type models. This simplified approach was taken in [1] (hereafter CS), where we studied the equilibration of a forced-dissipated two-level quasigeostrophic flow in both Cartesian and spherical geometry. The study showed that, in the simplified context, two main mechanisms were responsible for limiting the growth of baroclinically unstable eddies and hence bringing the system to equilibrium.

(*) The authors of this paper have agreed to not receive the proofs for correction.

The first,"baroclinic adjustment" [2], is due simply to the depletion of zonal-mean available potential energy (APE), which is consumed by the baroclinic growth of the eddy. When APE falls bellow a certain threshold (corresponding to the transition between baroclinically stable to unstable conditions) the wave is no longer able to extract APE from the mean flow and growth ceases. If this were the only operative mechanism, we would expect the equilibrated temperature gradient (that is, the time-mean meridional temperature gradient of the forced-dissipated system) to be fairly independent of the forcing temperature gradient, since the instability threshold is an intrinsic characteristic of the wave and does not depend on the forcing applied to the mean flow.

However, it was found in CS that a second growth-limiting mechanism is also important. This is the "barotropic governor" effect [3], which consists in the production of strong meridional wind shear by the convergence of the eddy momentum flux; the presence of this shear conditions the meridional structure of the wave and limits the efficiency with which it can extract APE from the zonal-mean flow [4]. In effect, the presence of meridional wind shear raises the threshold for baroclinic instability. As the forcing temperature gradient increases, so does the mean amplitude of the wave, which is able to induce an ever higher level of meridional shear in the zonal-mean wind. As a result, the equilibrated temperature gradient, which roughly follows the instability threshold, tends to increase with the forcing.

It was also found in CS that the role of the barotropic governor was considerably more pronounced in spherical than in Cartesian geometry, because the intrinsic tendency of the eddies to transport momentum northward induced high levels of momentum convergence near the northern channel margin, giving rise to a rather sharp jet pressed against the channel wall. Naturally, the presence of a rigid lateral boundary is an unrealistic feature. The doubt remains that if the wall were removed, the equilibrated jet could prove to be much less sharp, with much weaker meridional wind shear, so that the barotropic governor would play a more marginal role. Further, it is well known [5, 6] that the zonally symmetric circulation will itself produce a jet, and it is not clear how this and the eddy-induced jet will interact.

Our purpose in the present paper is to extend the study of CS to the somewhat more realistic case of a primitive equation (PE) model on the entire sphere (instead of a channel on the sphere as in CS). We are thus able to generate a more realistic zonally symmetric basic state, and we avoid the problem of rigid side walls. We will however retain other simplifying features of CS, notably a two-level vertical discretisation, restriction of the number of baroclinically active waves by including only integer multiples of wave number 3, and Newtonian cooling to parameterise diabatic heating.

2. – The model

We use the dry primitive equations written in pressure coordinates [7]:

$$\frac{\mathrm{d}\mathbf{u}}{\mathrm{d}t} = -f\mathbf{k}\times\mathbf{u} \; - \nabla\Phi \; + \frac{\partial}{\partial p}\left(\nu\frac{\partial \mathbf{u}}{\partial p}\right) \; - \gamma\nabla^8\mathbf{u}\,, \tag{1}$$

$$\frac{\mathrm{d}\theta}{\mathrm{d}t} = -\alpha(\theta-\theta^\star) \; - \gamma\nabla^8\theta\,, \tag{2}$$

$$0 = \nabla\cdot\mathbf{u} \; + \; \frac{\partial\omega}{\partial p}\,, \tag{3}$$

$$\frac{\partial\Phi}{\partial\zeta} = -C_p\theta\,, \tag{4}$$

where $\mathbf{u} = (u, v)$ is the horizontal wind, θ is potential temperature, $\zeta \equiv (p/p_s)^\kappa$ and ∇ is the horizontal gradient; other symbols have their usual meteorological meaning. We include internal vertical friction with coefficient ν. Surface friction is represented by a linear term of the form $-r\mathbf{u}$ in the lowest layer only. Horizontal hyper-diffusion with coefficient γ is included so as to prevent accumulation of enstrophy at the shortest scales. The temperature field is relaxed towards an axially symmetric "radiative-convective equilibrium" $\theta^\star$ of the form used by Held and Hou [6]:

$$\theta^\star \;=\; \Theta(p) \;+\; \frac{1}{2}\Delta\theta^\star \left(\cos\ 2\varphi + \frac{1}{3}\right),$$

where φ is latitude, $\Theta(p)$ gives the vertical stratification and $\Delta\theta^\star$ gives the forcing equator-to-pole temperature difference. The model is vertically discretised into two levels (250 and 750 hPa) following the energy-conserving scheme of Lorenz [8]. In the horizontal, the model is fully spectral. Throughout the study, we employ a horizontal resolution of T42, but including only zonal wave numbers which are multiples of 3; this is done in order to enable comparison with the results of CS. The numerical implementation is due to R. Saravanan, who has studied the behaviour of this model in some detail [9]. Note that the "superrotating" regime studied by Saravanan is not relevant here since our forcing is purely zonally symmetric.

Fixed parameter values include $r = 0.18 \times 10^{-6}$ s^{-1} (6 day Rayleigh friction), $\alpha = 2 \times 10^{-7}$ s^{-1} and γ such that the smallest wave is damped on a timescale of a few hours. Θ is chosen to be 285 K in the lower layer and 30 K higher in the upper layer. The parameters $\Delta\theta^\star$ and ν will be varied as discussed below.

We note that the value of α employed here corresponds to a 58-day Newtonian cooling time scale. Although there is some uncertainty as to what the "right" cooling time scale should be, a general consensus sets it somewhere in the neighbourhood of 20 days, so the value employed here should be viewed as unrealistically long. The reason why we use this value is simply to compare with the results of CS, who in turn used this value to compare with the earlier work of [10]. As noted in CS, the sensitivity of the results to changes in α is certainly an interesting question, which we plan to address in future work. However, we feel it is outside the scope of the present brief contribution.

3. – Results

If all zonally asymmetric components in the model are constrained to be zero, then the model develops a purely symmetric circulation of the type discussed by Held and Hou [6]. We shall refer to this as the "Hadley state". When there is no friction between the two layers ($\nu = 0$), a pure superrotation is obtained. If some internal viscosity is present, a Hadley circulation develops. The Hadley cell tends to flatten out the temperature gradient in the tropical region, thus in effect reducing the overall equator-to-pole temperature difference; we denote this mean meridional temperature gradient in the Hadley state by $\Delta\theta_{\mathrm{H}}$. The zonal wind in balance with this temperature field will be close to zero near the equator and present a baroclinic jet at the poleward margin of the Hadley cell, where the temperature gradient is steepest. As an example, we present in fig. 1 the zonal wind in the Hadley state for $\Delta\theta^\star = 50$ K. For $\nu = 0$, a pure superrotation is obtained in the upper layer with zero wind in the lower layer (because of surface friction). When internal friction is present, a subtropical jet is formed, becoming broader and weaker as ν increases. These results are very similar to those found in a multi-layer model in [6].

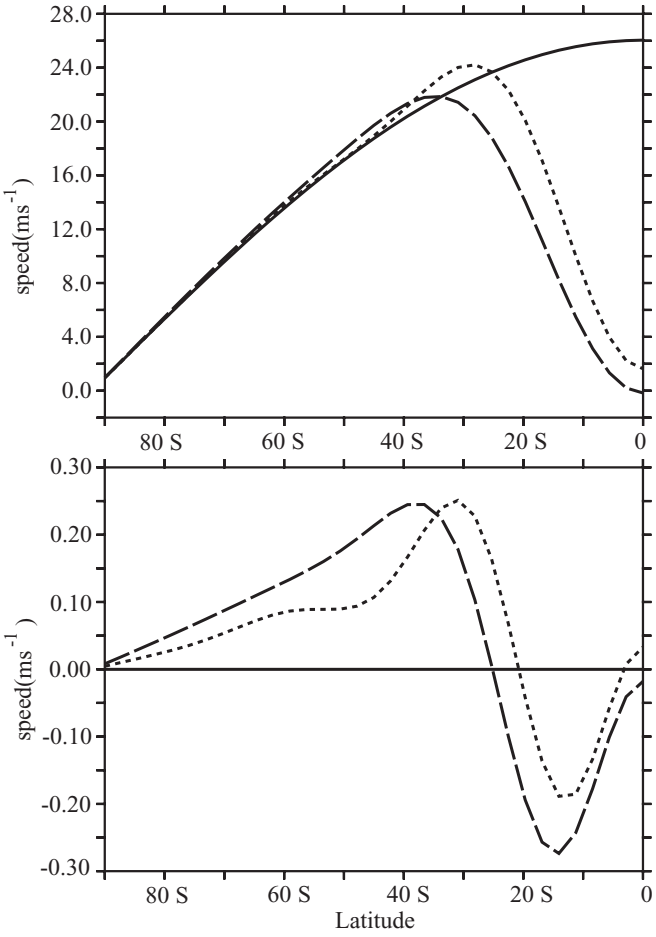

Fig. 1. – Zonal wind in the Hadley state for $\Delta\theta^\star = 50$ K. The upper (lower) panel refers to the upper (lower) model layer. Three values of ν are used: 0 (solid line), 5 (dotted line) and 15 m^2 s^{-1} (dashed line). Units are m s^{-1}.

For values of $\Delta\theta^\star$ greater than 20 K, the Hadley state turns out to be baroclinically unstable for all reasonable values of ν. Initially small zonally asymmetric perturbations will grow to finite amplitude, transporting heat polewards and hence reducing the mean meridional temperature gradient. This tendency will be opposed by the diabatic forcing, which acts to replenish the temperature gradient. The final equator-to-pole temperature difference $\Delta\theta_{\rm e}$ will be a trade-off between the opposing tendencies of the eddies and the forcing. Asymptotically, the system can settle into either a steady state (in which the eddy heat flux convergence exactly matches the diabatic forcing) or into a periodic or randomly fluctuating state, in which the equilibration is only statistical. In any case, we refer to this asymptotic state as the "equilibrated state".

To study the equilibrated state, we first spin the model up into the Hadley state, keeping all wave components set to zero. Once the model has converged to the Hadley state, we introduce small zonally asymmetric perturbations and allow them to grow and evolve freely for 1500 days. Statistics of the equilibrated state are taken over the last

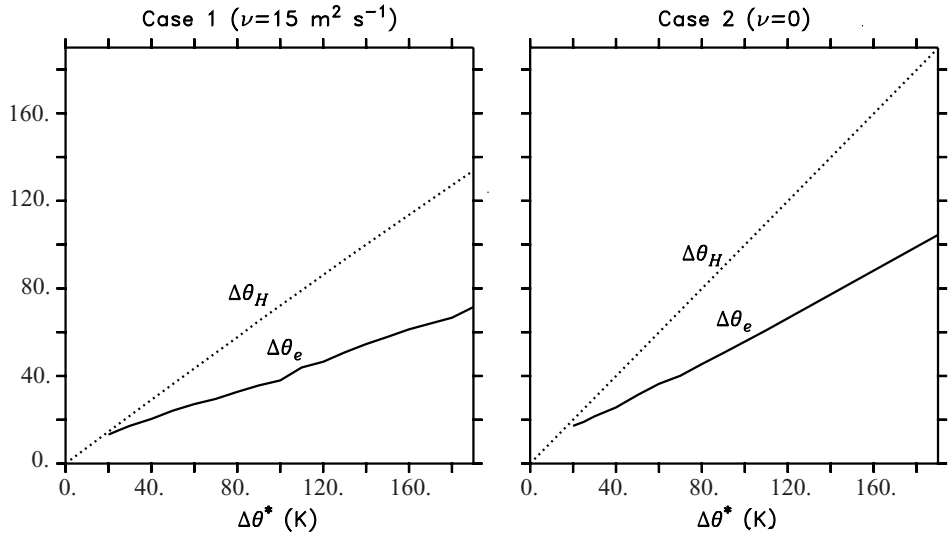

Fig. 2. – The mean equator-to-pole temperature difference in the Hadley state ($\Delta\theta_{\rm H}$) and in the equilibrated state ($\Delta\theta_{\rm e}$) as a function of the forcing equator-to-pole temperature difference $\Delta\theta^\star$. Units are K.

1000 days of the run. This procedure is repeated for a range of values of $\Delta\theta^\star$. We examine two cases: a viscous case (case 1), where $\nu = 15$ m^2 s^{-1}, and an "inviscid" case (case 2), in which $\nu = 0$; note, however, that case 2 is not truly inviscid since bottom friction is still active.

3˙1. *Presence of the barotropic governor effect.* – As discussed in the introduction, one of the ways in which the barotropic governor manifests itself is by making the equilibrated temperature gradient sensitive to the forcing. Figure 2 shows that in both case 1 and 2 the equilibrated temperature gradient increases rapidly with $\Delta\theta^\star$, suggesting that the barotropic governor plays a relevant role in both cases. In the range of forcing studied, $\Delta\theta_{\rm e}$ appears to be a linear function of $\Delta\theta^\star$. This essentially linear dependence was also found in CS, though over a narrower range of forcings: at high forcings, a new regime appeared in which the $\Delta\theta_{\rm e}$ curve was almost flat. Such a regime may possibly exist also in the present model, but at forcings which appear unrealistically high.

Direct examination of the zonal-mean zonal wind, figs. 3 and 4, shows that in both case 1 and 2 the equilibrated state features a rather sharp mid- to high-latitude jet, which becomes more intense and shifts further polewards as the forcing increases. Note that even at low forcings the jet axis is well polewards of 40° latitude. Examination of the zonal-mean meridional and vertical wind fields (not shown) indicates that at all levels of forcing the Hadley cell's poleward margin lies between 30° and 40°. Thus, the jet maximum in the equilibrated state is not associated with the Hadley cell. Rather, the edge of the Hadley cell shows up in the zonal-mean wind as a slight hump or secondary maximum in the subtropical upper level wind, which is particularly clear at low forcing.

It is of interest in this context to examine the maintenance of the zonal wind in more detail. It is easy to show from (1) that

$$\frac{\partial \overline{u}}{\partial t} \;=\; \left(f + \overline{\zeta}\right)\overline{v} \;+\; \mathrm{conv}\left(\overline{u'v'}\right) \;+\; \text{other terms}, \tag{5}$$

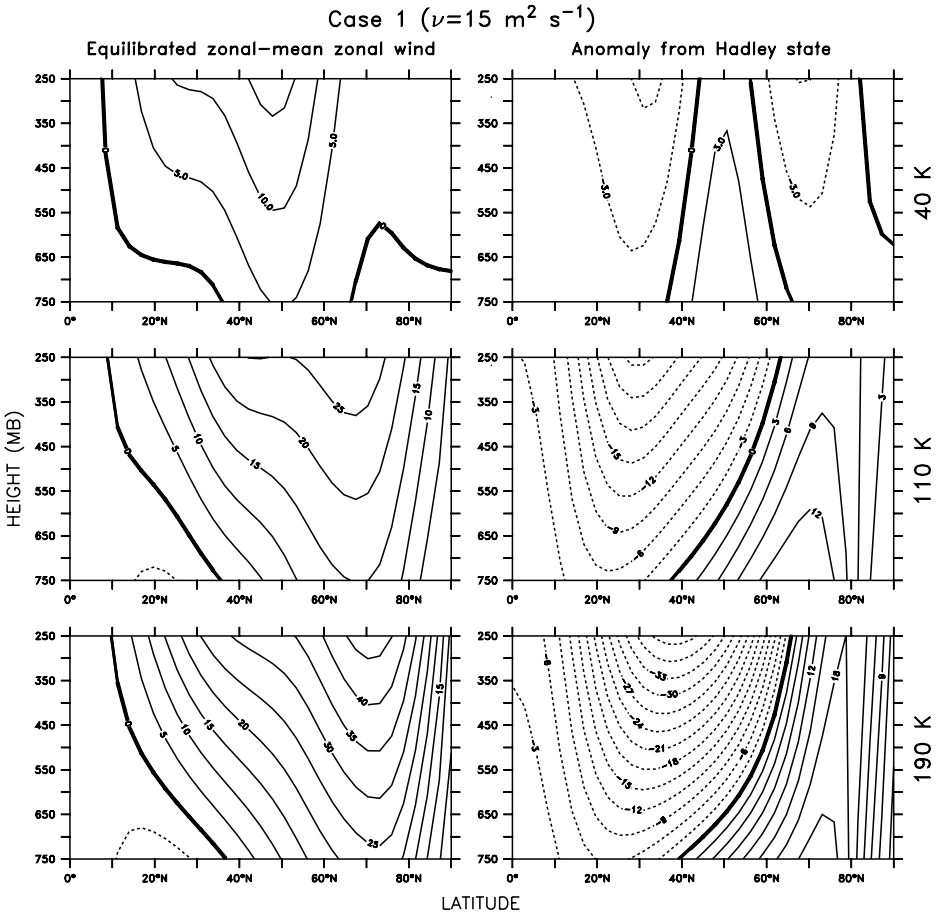

Fig. 3. – The time- and zonal-mean zonal wind in the equilibrated state (left, contours every 5 m s^{-1}) and its difference from the Hadley state (right, contours every 3 m s^{-1}) in the viscous case (case 1) for three values of the forcing equator-to-pole temperature difference $\Delta\theta^\star$: 40 K (top), 110 K (middle) and 180 K (bottom). Negative contours are dashed. Note that the fields in the figures are only specified at two levels (250 and 750 mb); the contour plots are obtained by feeding these values to a standard plotting package which employs cubic spline interpolation. Thus the detailed shapes of the contours should not be taken too seriously; only the general position and strength of the maxima are of interest.

where $\overline{()}$ and $()'$ represent the zonal average and the deviation therefrom, ζ is the relative vorticity, and the "other terms" describe vertical convergence and dissipation and are generally much smaller than the first two (though dissipation can be important in the lower layer). The first term on the RHS of (5) represents the effect of the mean meridional circulation (the Hadley and Ferrel cells) while the second term,

$$\mathrm{conv}\left(\overline{u'v'}\right) \;=\; -\frac{1}{a\cos^2\varphi}\frac{\partial}{\partial\varphi}\left(\cos^2\varphi\,\overline{u'v'}\right)\,,$$

describes the eddy momentum flux convergence. Both terms are plotted in fig. 5 for each

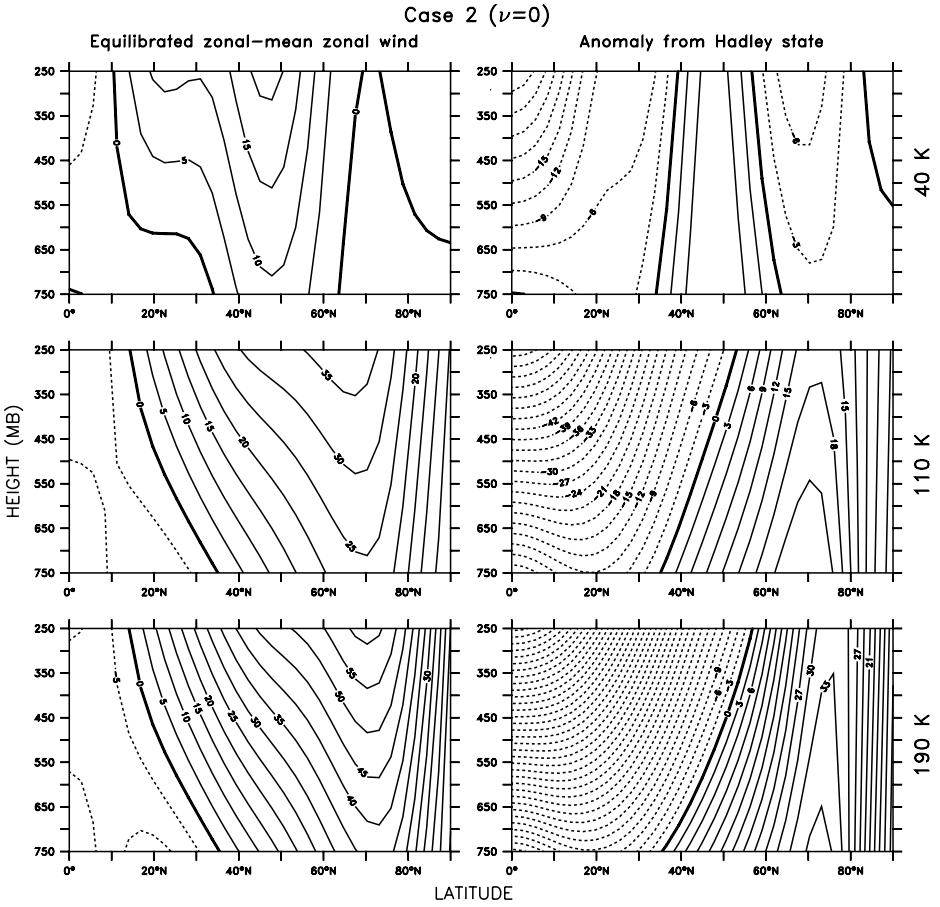

Fig. 4. – As in fig. 3 but in the case with no internal viscosity (case 2).

of the cases portrayed in figs. 3 and 4. Clearly, between 0° and 40° the Hadley cell is driving the westerly wind, while the eddies are retarding it, while polewards of 40° the situation is exchanged with the eddies driving the jet, while the Ferrel cell decelerates it. In other words, the strong mid-latitude jet is due to the eddy momentum flux, while the Hadley cell accounts for the small subsidiary maximum in the subtropics.

Returning to figs. 3 and 4, we see also (right-hand panels) that, in the region where the eddies are driving the jet (*i.e.* polewards of 40°), their effect is to add a barotropic component to the pre-existing symmetric circulation (note in fact that the contour lines of the anomalous flow are almost vertical at mid and high latitudes). It is this barotropic, meridionally sheared component of the flow that gives rise to the barotropic governor effect.

3˙2. *Effect of internal viscosity.* – While the presence of internal viscosity has a dramatic effect on the Hadley state (see fig. 1), the effect is less clear in the equilibrated state. Note indeed how similar the viscous zonal-mean flows of case 1 (fig. 3) are to their inviscid counterparts (fig. 4). On the other hand, fig. 2 shows that $\Delta\theta_{\mathrm{e}}$ grows more rapidly in case 2 than in case 1, which might tempt us to conclude that the barotropic governor is stronger in the inviscid case. However, we should note that $\Delta\theta_{\mathrm{H}}$ also grows more rapidly

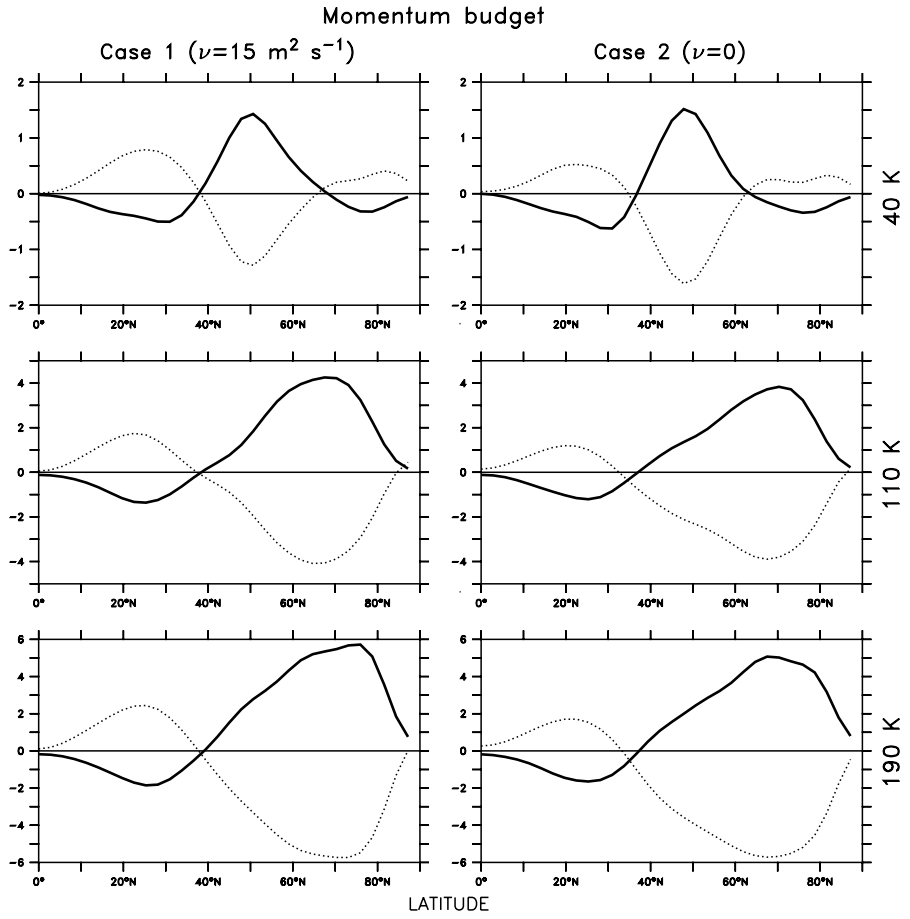

Fig. 5. – Leading terms in the maintenance of the equilibrated zonal-mean wind in the upper layer in the viscous (left) and inviscid (right) cases: eddy momentum convergence conv $\left(\overline{u'v'}\right)$ (solid line) and mean meridional circulation term $\left(f+\overline{\zeta}\right)\overline{v}$ (dotted line). Units are m s^{-1} day^{-1}.

in case 1. More precisely, in case 1 the slope of $\Delta\theta_{\mathrm{H}}$ is about 0.72 while that of $\Delta\theta^{\star}$ is about 0.33; the respective values for case 2 are 1 and 0.47. The ratio of the two slopes is about 2.1 in both cases. This suggests that the role of internal viscosity is to *rescale* the forcing temperature gradient: it is as if, in the presence of internal viscosity, the temperature gradient towards which the model relaxes is effectively $\Delta\theta_{\mathrm{H}}$ rather than $\Delta\theta^{\star}$.

Further evidence in this respect may be obtained by examining the eddy heat fluxes separated by wave number, as shown in fig. 6. Clearly, in both case 1 and 2, waves 3, 6 and 9 play a comparable role at low forcing. As the forcing increases, wave 9 and then wave 6 saturate, their respective heat fluxes stabilising at a more or less constant value [10]. We note firstly that the level at which the heat fluxes saturate is roughly the same in both cases: about 2 K m s^{-1} (0.5 K m s^{-1}) for wave 6 (9). On the other hand, the value of $\Delta\theta^{\star}$ at which a given wave saturates is considerably higher in case 1 than in case 2. Specifically, wave 6 begins to saturate at around $\Delta\theta^{\star}=80$ K in case 1, while in case 2 the value is closer to 60 K. However, referring to fig. 2, we see that in case 1 $\Delta\theta^{\star}=80$ K corresponds to roughly $\Delta\theta_{\mathrm{H}}=60$ K. A similar correspondence holds for

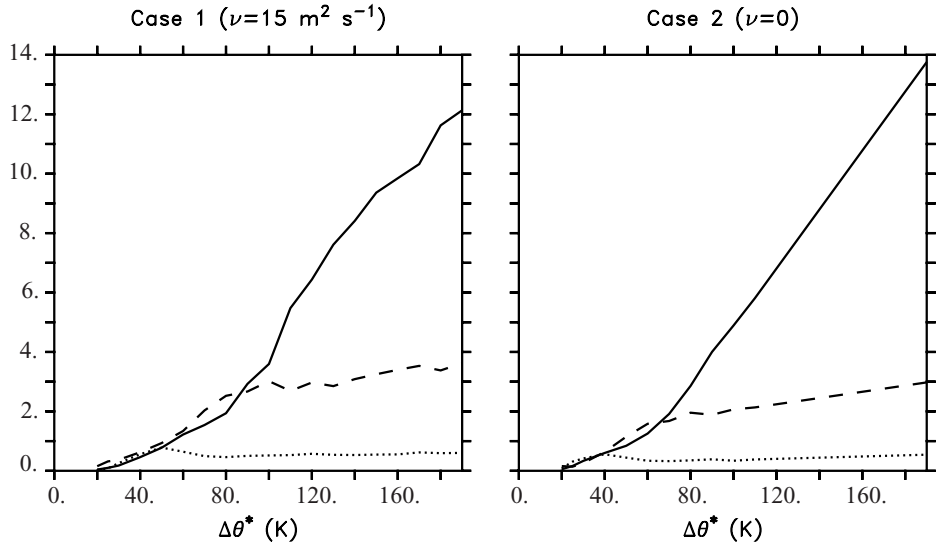

Fig. 6. – Hemispheric mean of the equilibrated poleward heat flux in the viscous (left) and inviscid (right) cases: wave 3 (solid line), 6 (dashed line) and 9 (dotted line) contributions. Units are K m s^{-1}.

wave 9. In other words, if we were to re-plot the heat flux curves for case 1 (fig. 6, left panel) using $\Delta\theta_{\mathrm{H}}$ rather than $\Delta\theta^{\star}$ as an abscissa, we would obtain a figure very similar to the corresponding one for case 2.

4. – Conclusions

We have studied the equilibration of a primitive equation model subject to forcing and dissipation. The forcing consists of a relaxation towards a given meridional temperature profile with equator-to-pole temperature difference $\Delta\theta^{\star}$. The damping consists in internal and bottom friction. Resolution is limited to two layers in the vertical and to zonal wave numbers which are integer multiples of 3. We find that in the presence of internal viscosity, the model exhibits an axially symmetric equilibrium with a Hadley circulation and a subtropical jet. When the non-symmetric components are included, the model develops a strong barotropic jet at mid-to-high latitudes which is driven by the eddy momentum convergence. The mean temperature gradient in the equilibrated state, $\Delta\theta_{\mathrm{e}}$, is found to rise almost linearly with the forcing. These qualitative results are valid whether internal viscosity is present or not.

This study leads us to two main conclusions:

i) The barotropic governor effect exerts an important influence on the equilibration of the model. In this sense, the present model is similar to the quasigeostrophic spherical model studied in CS.

ii) The effect of introducing internal viscosity is to give an effective forcing temperature gradient which is close to $\Delta\theta_{\mathrm{H}}$, the equator-to-pole temperature gradient in the axially symmetric equilibrium. This is a tentative conclusion; further experimentation is required to set it on a firmer basis.

One of the questions we set out to answer in this study was whether the rigid channel side walls present in CS were essential in order to obtain a strong barotropic governor effect. The answer appears to be no, since there are no artificial side walls in the present model. Rather, it appears that the pole (which is a turning point in the WKB sense) itself acts as a natural boundary, allowing the formation of a strong barotropic jet. We note that this is not as unrealistic a feature as may appear at first sight, since a jet axis polewards of 40° latitude is commonly observed in the Southern Hemisphere, particularly in spring and autumn. In the Northern Hemisphere, on the other hand, the jet axis is more nearly subtropical. This inter-hemispheric difference is most likely linked to the differences in surface properties in the two hemispheres (orographic forcing, land-sea contrasts etc.). We remark also that our results indicate that a low-latitude Hadley circulation can be induced as an effect of the large-scale baroclinic eddies, regardless of whether an internal dissipation mechanism is acting upon the system. These issues deserve further study.

* * *

We would like to thank R. SARAVANAN for making his primitive equation code available. The first author (RC) was supported by Danmarks Grundforskningsfond. AS was supported by the European Commission under contract ENV4-CT98-0733.

REFERENCES

[1] CABALLERO R. and SUTERA A., *J. Atmos. Sci.*, **57** (2000) 3296.
[2] STONE P. H., *J. Atmos. Sci.*, **35** (1978) 561.
[3] JAMES I. N. and GRAY L. J., *Quart. J. R. Meteor. Soc.*, **112** (1986) 1231.
[4] JAMES I. N., *J. Atmos. Sci.*, **44** (1987) 3710.
[5] SCHNEIDER E. K., *J. Atmos. Sci.*, **34** (1977) 280.
[6] HELD I. M. and HOU A. Y., *J. Atmos. Sci.*, **37** (1980) 515.
[7] PHILLIPS N. A., *Principles of Large Scale Weather Prediction*, in *Dynamic Meteorology*, edited by P. MOREL (Reidel, Dordrecht) 1973.
[8] LORENZ E. N., *Tellus*, **XII** (1960) 364.
[9] SARAVANAN R., *J. Atmos. Sci.*, **50** (1993) 1211.
[10] WELCH W. T. and TUNG K. K., *J. Atmos. Sci.*, **55** (1998) 1285.